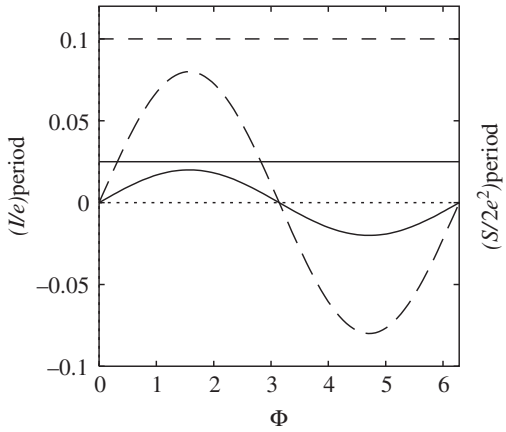

Fig. 1.50. Example: current and noise for a small pumping cycle described in the text. The horizontal lines represent noise, which does not depend on Φ. The curves denote the current, which is an oscillating function of Φ. The parameter η differs for dashed ($\eta = 0.05$) and solid ($\eta = 0.2$) curves, respectively. All other parameters are the same: $T = R = 0.5$, $r = 0.1$.

1.8 Andreev scattering

In this section, we consider electron transport in nanostructures which are connected not only to the reservoirs in the normal state, but also to one or several reservoirs that are in the superconducting state. Electron properties of superconductors differ from those of normal metals, as explained in Appendix B. The energies of the quasiparticle states are separated from the Fermi energy by the superconducting gap Δ. Let us count energy measured from the Fermi level. If a piece of a normal metal is brought into a contact with a superconductor, an electron with an energy above Δ can enter the superconductor, where it will be converted into a quasiparticle of the same energy. This, however, does not work at $E < \Delta$ since there are no quasiparticles. Therefore, for voltages and temperatures below Δ, no current may flow to the superconductor according to the scattering approach considered in the preceding sections.

1.8.1 Andreev reflection

Charge transfer may proceed, however, by a different mechanism: an electron coming from a normal metal to a superconductor can be reflected back as a hole. While this process conserves energy, it does not conserve charge in the normal metal: since the charges of an electron and a hole are opposite, a charge deficit of $2e$ arises. This implies that a Cooper pair with charge $2e$ has been added on the superconducting side. This transfers the charge from the normal metal into the superconductor. Let us note that the momentum of the hole $\hbar k_\mathrm{h}$ is almost equal to that of the electron, $\hbar k_\mathrm{h} = \hbar k_\mathrm{e} - 2E/v_\mathrm{F}$ (Fig. 1.51). Since $|E| \ll E_\mathrm{F}$, $k_\mathrm{h} \approx k_\mathrm{e} \approx k_\mathrm{F}$. However, the velocity of the holes, $v_\mathrm{h} = \hbar^{-1}(\partial E/\partial k_\mathrm{h})$ is opposite to that of electrons; holes with $k_\mathrm{h} > 0$ actually move away from the superconductor. This process is called *Andreev reflection* [29].

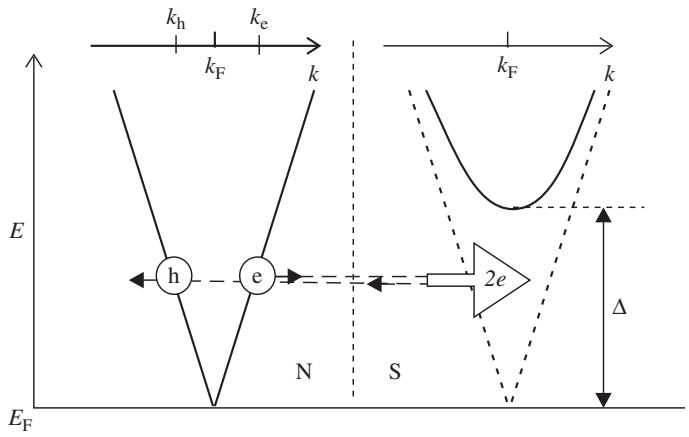

Fig. 1.51. Andreev reflection: an electron coming from a normal (N) metal to a superconductor (S) is reflected as a hole with the same energy and approximately the same momentum.

Let us elaborate on the quantitative description of Andreev reflection. In the presence of superconductivity, an excitation in a metal is conveniently represented by a *two-component* wave function, the components describing electrons ($\psi_e(\boldsymbol{r})$) and holes ($\psi_h(\boldsymbol{r})$). The wave function obeys the *Bogoliubov – de Gennes* (BdG) *equation*, which is a generalization of the Schrödinger equation:

$$\begin{pmatrix} \hat{H} & \Delta e^{i\varphi} \\ \Delta e^{-i\varphi} & -\hat{H}^* \end{pmatrix} \begin{pmatrix} \psi_e(\boldsymbol{r}) \\ \psi_h(\boldsymbol{r}) \end{pmatrix} = E \begin{pmatrix} \psi_e(\boldsymbol{r}) \\ \psi_h(\boldsymbol{r}) \end{pmatrix}. \tag{1.156}$$

Here the energy is counted from the Fermi level, so that $\hat{H} = \hat{H}_0 - E_F$, $\hat{H}_0 = -(\hbar^2/2m)(\nabla + ie\boldsymbol{A}(\boldsymbol{r})/\hbar c)^2 + U(\boldsymbol{r})$ being the Hamiltonian for electrons in the absence of any superconductors. As explained in Appendix B, the superconductivity mixes electrons and holes. With these cross-terms, the Hamiltonian becomes a 2×2 matrix. The cross-terms are off-diagonal elements of the matrix and are complex numbers with modulus Δ and phase φ. These values are position-dependent and vanish in the normal part of the nanostructure. It is enough for our purposes to assume that Δ and φ are constant in the superconducting reservoir, with Δ being equal to the superconducting energy gap far in the reservoir.[6]

To understand the meaning of Eq. (1.156), let us first consider a normal metal, in which the Hamiltonian is diagonal and the equations for the electron and hole components separate. The solutions are plane waves $\psi_{e,h}(\boldsymbol{r}) \propto \exp(i\boldsymbol{kr})$. Substituting this into Eq. (1.156), and considering only excitations close to the Fermi surface, $|E| \ll E_F$, we find $k = k_F \pm E/\hbar v_F$, where $\pm$ represents electron and hole components, respectively. Note that the momenta of both electron-like and hole-like solutions can be either above or below k_F. This is in conflict with the conventional definition of quasiparticles in a normal metal,

[6] Strictly speaking, the values of $\Delta(\boldsymbol{r})$ and $\varphi(\boldsymbol{r})$ actually depend on the solutions of BdG equations at all energies. Consequently, the superconducting pair amplitude Δ is suppressed in the region adjacent to the normal reservoir. However, the suppression does not play an important role and can be disregarded for model purposes [30].

where the quasiparticles with $k > k_F$ ($k < k_F$) are called electrons (holes). We can easily sort out this problem for the normal metal. Indeed, BdG equations allow for solutions with positive energies, $E = |\xi|$, where we have defined $\xi = \hbar v_F(k - k_F)$, as well as for the solutions with negative energies, $E = -|\xi|$. The latter are not independent from the former; they are obtained from each other by a flip of components. Thus, BdG equations contain a double set of solutions. The solutions with negative energies would represent electrons with $k < k_F$ and holes with $k > k_F$ – contradicting the conventional definition of a quasiparticle. To conform to the conventional definition of electrons and holes in a normal metal, we retain the solutions with positive energies only.

Let us now look at the solutions of Eq. (1.156) in a superconductor. Substituting $\psi_{e,h}$ in the form of plane waves and assuming $\Delta, E \ll E_F$, we find that the corresponding energies are given by

$$E = \sqrt{\xi^2 + \Delta^2}, \quad \xi = \hbar v_F(k - k_F). \tag{1.157}$$

For $E > \Delta$, quasiparticles can freely propagate in a superconductor and have an energy spectrum given by Eq. (1.157) rather than $E = |\xi|$. For $E < \Delta$, quasiparticles in a bulk superconductor do not exist.

We consider next an *ideal* (no scattering) contact between a normal metal ($x < 0$) and a superconductor ($x > 0$). Since the transport channels are not mixed, it suffices to consider one transport channel n (this channel index will be suppressed where it does not lead to the confusion). Let us look at the solutions of the form $\psi_{e,h}(x) \propto \tilde{\psi}_{e,h}(x) \exp(\mathrm{i}k_F^{(n)}x)$ that correspond to an electron propagating to the right and a hole moving in the opposite direction. The envelope function $\tilde{\psi}(x)$ varies at a space scale that is much bigger than the electron wavelength and satisfies the following BdG equation:

$$\begin{pmatrix} -\mathrm{i}\hbar v_F\, \mathrm{d}/\mathrm{d}x & \Delta(x)\mathrm{e}^{\mathrm{i}\varphi} \\ \Delta(x)\mathrm{e}^{-\mathrm{i}\varphi} & \mathrm{i}\hbar v_F\, \mathrm{d}/\mathrm{d}x \end{pmatrix} \begin{pmatrix} \tilde{\psi}_e(x) \\ \tilde{\psi}_h(x) \end{pmatrix} = E \begin{pmatrix} \tilde{\psi}_e(x) \\ \tilde{\psi}_h(x) \end{pmatrix}. \tag{1.158}$$

In the normal metal, we take the wave function in the form

$$\tilde{\psi}(x < 0) = \begin{pmatrix} \mathrm{e}^{\mathrm{i}xE/\hbar v_F} \\ r_A \mathrm{e}^{-\mathrm{i}xE/\hbar v_F} \end{pmatrix}, \tag{1.159}$$

which describes the incoming electron and the outgoing Andreev-reflected hole. The hole amplitude acquires an extra factor r_A: the amplitude of Andreev reflection.

For $E < \Delta$, there are no solutions extending to the bulk of the superconductor. There is, however, an *evanescent* solution falling off away from the normal reservoir. This is given by

$$\tilde{\psi}(x > 0) = C \begin{pmatrix} f_e \\ f_h \end{pmatrix} \mathrm{e}^{-x\sqrt{\Delta^2 - E^2}/\hbar v_F}, \tag{1.160}$$

where C is an arbitrary constant and the coefficients $f_{e,h}$ are to be found from Eq. (1.158) (the BdG equation) and the normalization condition $|f_e|^2 + |f_h|^2 = 1$.

Control question 1.20. What are the explicit forms of $f_{e,h}$?

The typical scale of penetration into the superconductor – the superconducting correlation length – is of the order $\hbar v_F/\Delta \gg \lambda_F$ and diverges at the threshold energy $E = \Delta$.

Now let us find the amplitudes r_A and C matching both solutions at $x = 0$. The derivatives do not have to be matched since the effective BdG equation contains the first derivatives only. The amplitude of Andreev reflection is given by

$$r_A(E) = e^{i\chi} = e^{-i\varphi}\left(\frac{E}{\Delta} - i\frac{\sqrt{\Delta^2 - E^2}}{\Delta}\right), \quad \chi = -\arccos\left(\frac{E}{\Delta}\right) - \varphi. \tag{1.161}$$

As expected, the electron is fully Andreev reflected ($|r_A|^2 = 1$). The phase of the outgoing hole is shifted by χ with respect to the phase of the incoming electron. The phase shift between the amplitudes of an incoming hole and an outgoing electron, calculated similarly, equals $\tilde{\chi} = -\arccos(E/\Delta) + \varphi$.

Exercise 1.17. (i) Write down the solutions of the BdG equation, Eq. (1.158), for energies above the threshold, $E > \Delta$. (ii) Matching these solutions with the solutions in the normal metal, show that the amplitude of Andreev reflection is given by

$$r_A = e^{-i\varphi}\left(\frac{E}{\Delta} - \frac{\sqrt{E^2 - \Delta^2}}{\Delta}\right). \tag{1.162}$$

(iii) Note that $|r_A|^2 < 1$ and describe the corresponding scattering process. (iv) Find the asymptotic expression for the probability of Andreev reflection for $E \gg \Delta$.

1.8.2 Andreev conductance

We now consider a more general situation in which a nanostructure is placed between the normal and superconducting reservoirs. The nanostructure in the normal state is described by a scattering matrix $\hat{s}(E)$ that generally depends on energy. Quite amusingly, the same scattering matrix determines the properties of Andreev reflection, which is now combined with the common "normal" reflection of electrons or holes coming to the nanostructure from either side. The scattering theory for Andreev reflection was first put forward by Blonder, Tinkham, and Klapwijk [31].

To start with, we have to find the scattering matrix for electrons and holes. For electrons at energy $E > 0$, this is obviously $\hat{s}_e(E) = \hat{s}(E)$. The holes at the same energy involve states below the Fermi level, and their scattering is related to $\hat{s}(-E)$. However, as we have seen, an electron and a hole at the same momentum have opposite velocities, so the incoming electrons correspond to outgoing holes and vice versa. To account for this, one replaces $\hat{s}$ by $\hat{s}^{-1}$. In addition, the holes obey a time-reversed Hamiltonian: to account for this, the scattering matrix must be transposed. Therefore,

$$\hat{s}_h(E) = (\hat{s}(-E)^{-1})^T = \hat{s}^*(-E). \tag{1.163}$$

Control question 1.21. Which property of the scattering matrix guarantees Eq. (1.163)?

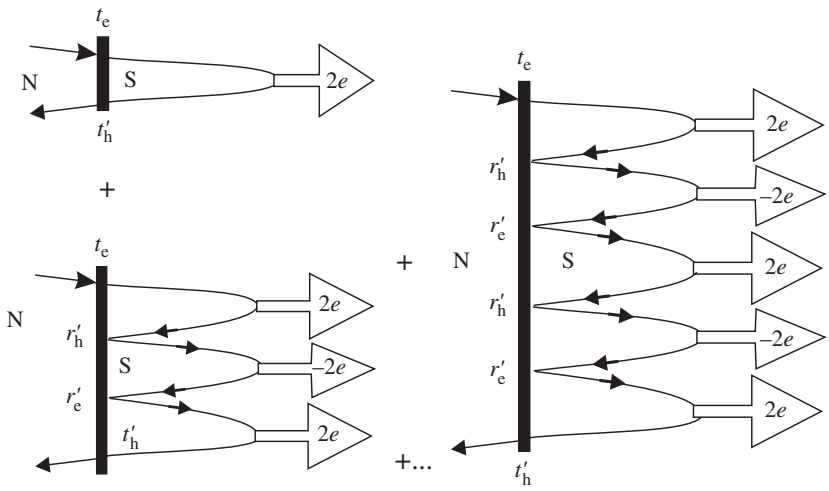

Fig. 1.52. **Andreev conductance. The amplitude of the Andreev equation to the normal (N) lead from the nanostructure adjacent to a superconductor (S) is contributed by the processes that differ in the number of electron trips between the nanostructure and superconductor.**

To simplify the notation, we consider a one-channel scatterer. For this setup, $r_e = r(E)$, $r_h = r^*(-E)$, $t_e = t(E)$, and $t_h = t^*(-E)$.

Let us calculate the amplitude of the Andreev reflection assuming $E < \Delta$. We use the same approach as in Section 1.6 to sum the amplitudes of various processes that convert the incoming electron to the outgoing hole (Fig. 1.52). The simplest process involves the electron transmission through the nanostructure (amplitude t_e), Andreev reflection from the superconductor (the phase factor $\exp(i\chi)$, see Eq. (1.161)) and transmission through the nanostructure in the backward direction as a hole (t'_h). Thus, the total amplitude of this process is given by $r_{a0} = t_e t'_h \exp(i\chi)$. The next process (Fig. 1.52) involves the reflection of the hole (amplitude r'_h). The hole is Andreev-reflected ($\exp(i\tilde{\chi})$), the resulted electron is reflected again (r'_e), and is converted back into a hole in the superconductor ($\exp(i\chi)$). Finally, the hole transmits through the nanostructure. The extra steps mentioned result in $r_{a1} = r_{a1} r'_h e^{i\tilde{\chi}} r'_e e^{i\chi}$. More complicated processes differ in the number of electron trips between the nanostructure and the superconductor, so that $r_{an} = r_{a0}(r'_h e^{i\tilde{\chi}} r'_e e^{i\chi})^n$. Summing them up, we obtain the total amplitude of Andreev reflection:

$$r_A = \sum_{n=0}^{\infty} r_{an} = \frac{t_e t'_h e^{i\chi}}{1 - r'_e r'_h e^{i(\chi+\tilde{\chi})}}. \tag{1.164}$$

Let us disregard the energy dependence of the scattering matrix: as we have seen, this is plausible if the energy scale associated with the dwell time in the nanostructure exceeds the energies involved, i.e. eV or Δ. In this case, the scattering matrices for electrons and holes are complex-conjugate.

To simplify, let us assume a low voltage $eV \ll \Delta$. We note that $\chi + \tilde{\chi} = -2\arccos(E/\Delta)$; since the relevant energies E are of the order of eV, one can approximate

$\chi + \tilde{\chi} = -\pi$. The Andreev reflection coefficient, $R_A = |r_A|^2$, is given by

$$R_A = \frac{T^2}{(2-T)^2}, \tag{1.165}$$

and is unambiguously determined by T, the transmission eigenvalue of the corresponding transport channel for the nanostructure in the normal state. The normal reflection coefficient is $R_N = 1 - R_A$. For ideal contact ($T = 1$), we recover the earlier result $R_A = 1$, $R_N = 0$. Note that the result in Eq. (1.165) is a consequence of quantum interference. A "classical" calculation (summing up the probabilities $|r_{an}|^2$ rather than the amplitudes) would yield a wrong result.

To calculate the conductance, we note the analogy with normal scattering. Indeed, the fraction R_N of incoming electrons is normally reflected; these electrons do not contribute to the current. The Andreev reflection process (probability R_A) results in the charge transfer of $2e$ (rather than e in the normal case). Thus, the *Andreev conductance* becomes $G_A = 2G_Q R_A$. The same reasoning actually reproduces the whole counting statistics of Andreev transport: it is given by the Levitov formula with $e \to 2e$ and $T \to R_A$.

Exercise 1.18. Determine the noise in Andreev transport. Express the result in terms of the Fano factor (see Eq. (1.64)). What is the upper boundary for the Fano factor?

For many transport channels, one obtains a sum over the channels:

$$G_A = 2G_Q \sum_p (R_A)_p = 2G_Q \sum_p \frac{T_p^2}{(2-T_p)^2}. \tag{1.166}$$

Now we can analyze this formula, employing the notion of the distribution of transmission eigenvalues.

Exercise 1.19. Assume that the nanostructure is diffusive so that the distribution of transmission eigenvalues is given by Eq. (1.43). Express the Andreev conductance in terms of the conductance in the normal state.

If the nanostructure is of a tunnel type, $T_p \ll 1$, we end up with $G_A = G_Q \sum_p T_p^2/2$. Andreev conductance is thus proportional to the second power of the transmission eigenvalues. This reflects the fact that Andreev reflection requires two transmission events, one of an electron and one of a hole. Note that in the normal state the conductance is much higher, being proportional to the first power of T_p. For an ideal contact ($T_p = 1$), the situation is reversed: $G_A = 2G$, the factor of 2 reflecting the fact that Andreev reflection transfers double charge.

1.8.3 Andreev bound states

Consider now a superconducting junction: a nanostructure placed between two superconductors that have the same superconducting gap Δ but differ in their phases. We assume

that the nanostructure is sufficiently short, not manifesting the energy dependence of its scattering matrix at energy scale Δ. Under these conditions, it is not important whether the nanostructure is made of a normal metal or a superconductor, or even an insulator. The absence of energy dependence implies that the electrons spend a very short time τ_d in the nanostructure; by virtue of the Heisenberg uncertainty principle, this time is too short to allow a response to the superconductivity inside the nanostructure, $\tau_d \Delta \ll \hbar$. The scattering matrix of the nanostructure is thus its scattering matrix in the normal state.

Let us consider an electron in the nanostructure at sufficiently low energy. It will experience Andreev reflections trying to get to either superconductor. The resulting hole experiences the same problem: it cannot escape the nanostructure and is converted back to an electron in the course of the escape attempt. We conclude that an electron/hole in the nanostructure must perform a so-called finite motion. Quantum mechanics teaches us that any finite motion of a particle gives rise to discrete energy levels. Indeed, a nanostructure between the superconducting reservoirs kept at different phases gives rise to a set of bound states for quasiparticles – *Andreev bound states*. Let us calculate the energies of these states.

First consider again a single channel. The scattering matrix of the nanostructure relates the amplitudes of outgoing and incoming states with respect to the nanostructure,

$$\begin{pmatrix} \boldsymbol{b}_e \\ \boldsymbol{b}_h \end{pmatrix} = \begin{pmatrix} \hat{s} & 0 \\ 0 & \hat{s}^* \end{pmatrix} \begin{pmatrix} \boldsymbol{a}_e \\ \boldsymbol{a}_h \end{pmatrix}, \tag{1.167}$$

where the two components of the amplitude vectors correspond to the left and right side of the nanostructure, respectively,

$$\boldsymbol{b}_e = \begin{pmatrix} b_{Le} \\ b_{Re} \end{pmatrix}; \quad \boldsymbol{b}_h = \begin{pmatrix} b_{Lh} \\ b_{Rh} \end{pmatrix},$$

and similarly for the incoming amplitudes $\boldsymbol{a}_e, \boldsymbol{a}_h$. The scattering of holes, as mentioned, is given by the complex-conjugate matrix $\hat{s}^*$. The nanostructure does not convert electrons to holes; this is why the matrix appearing in Eq. (1.167) is block-diagonal.

Andreev reflection from the superconductors converts electrons to holes and vice versa, yielding the following complementary relation between $\boldsymbol{a}$ and $\boldsymbol{b}$:

$$\begin{pmatrix} \boldsymbol{a}_e \\ \boldsymbol{a}_h \end{pmatrix} = \begin{pmatrix} 0 & \hat{s}_{eh} \\ \hat{s}_{he} & 0 \end{pmatrix} \begin{pmatrix} \boldsymbol{b}_e \\ \boldsymbol{b}_h \end{pmatrix}, \tag{1.168}$$

with

$$\hat{s}_{eh} = \begin{pmatrix} e^{i\tilde{\chi}_L} & 0 \\ 0 & e^{i\tilde{\chi}_R} \end{pmatrix}; \quad \hat{s}_{he} = \begin{pmatrix} e^{i\chi_L} & 0 \\ 0 & e^{i\chi_R} \end{pmatrix}.$$

The Andreev reflection phases are given by Eq. (1.161): $\chi_{L,R} = -\varphi_{L,R} - \arccos(E/\Delta)$, $\tilde{\chi}_{L,R} = \varphi_{L,R} - \arccos(E/\Delta)$, $\varphi_{L,R}$ being the superconducting phases of the left and right reservoirs.

Control question 1.22. Explain the structure of the matrix in Eq. (1.168).

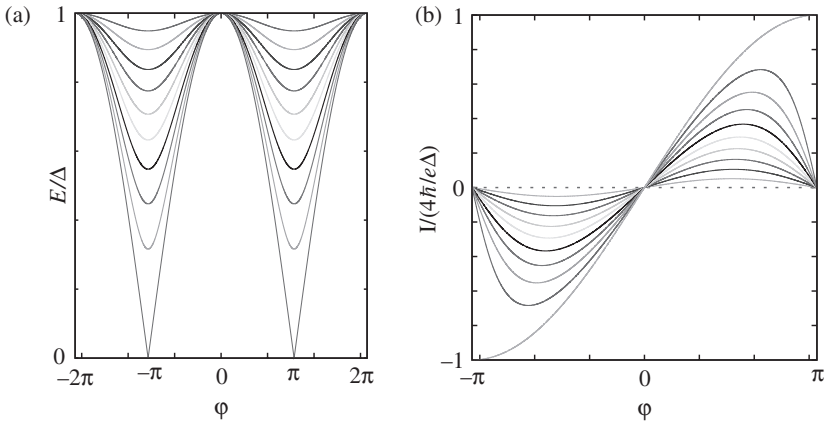

Fig. 1.53. (a) The energies of Andreev bound states versus φ for T_p, ranging from 0.1 (upper curve) to 1 (lowest curve) with step 0.1. (b) Corresponding superconducting currents (the upper curve at positive φ corresponds to $T_p = 1$).

Two systems of linear equations, Eqs. (1.167) and (1.168), have non-zero solutions only if the product $\hat{\Pi}$ of the 4×4 matrices in these relations has an eigenvalue 1. Indeed, if one excludes $\boldsymbol{a}$ from the equations, the equation for $\boldsymbol{b}$ reduces to the eigenvalue problem $\hat{\Pi}\boldsymbol{b} = \boldsymbol{b}$, and solutions exist only if $\det(\hat{\Pi} - \hat{1}) = 0$. Transforming this condition, one obtains the energy of the bound state:

$$E = \Delta\sqrt{1 - T\sin^2(\varphi/2)}, \tag{1.169}$$

where T is the transmission eigenvalue corresponding to the scattering matrix $\hat{s}$, and $\varphi = \varphi_{\mathrm{L}} - \varphi_{\mathrm{R}}$ is the phase difference across the junction [32].

Control question 1.23. Can you trace how Eq. (1.169) emerges from the conditions imposed on the Andreev phases $\chi_{\mathrm{L,R}}$?

For many channels, an Andreev bound state appears in each channel with the energy given by

$$E_p = \Delta\sqrt{1 - T_p\sin^2(\varphi/2)}. \tag{1.170}$$

The energy is modulated by the phase difference φ. For $\varphi = 0$, $E_p = \Delta$ for all channels. In this case, the states are not really bound: they are at the edge of a continuous quasiparticle spectrum in the superconductor. The minimum value $\Delta\sqrt{1 - T_p}$ is achieved at $\varphi = \pi$ (Fig. 1.53).

1.8.4 Josephson effect

So far we have considered the bound states for excitations. For example, an excitation can be a quasiparticle cooled down in the vicinity of the nanostructure: it will be trapped in the

bound state. An important property of superconductivity is the correspondence between the properties of the excitations and those of the ground state of the superconductor. This is manifested in the symmetry of the BdG equation with respect to positive and negative energies. The solutions at negative energies can be associated with the filled levels contributing to the ground-state energy, which is the sum of single-particle excitation energies E_n, $E_g = -\sum E_n$.[7]

Let us now concentrate on the ground-state energy of the system. It is contributed to by all excitation energies: those corresponding to propagating quasiparticles above the superconducting gap and those of the bound Andreev states. Only the latter contributions depend on the superconducting phase difference between the reservoirs φ. We concentrate on this phase-dependent part:

$$E(\varphi) = \sum_p E_p(\varphi) = \Delta \sum_p \sqrt{1 - T_p \sin^2(\varphi/2)}. \tag{1.171}$$

We will see now that the phase-dependent energy gives rise to a persistent current in the ground state – a *supercurrent*. Let us slowly vary the phase difference. The energy shift per unit time is given by

$$\frac{\mathrm{d}E}{\mathrm{d}t} = \frac{\partial E(\varphi)}{\partial \varphi}\frac{\mathrm{d}\varphi}{\mathrm{d}t}.$$

The global gauge invariance (see Appendix B) dictates that the time derivative of the superconducting phase is simply the potential of the corresponding superconductor, $\dot{\varphi} = 2eV/\hbar$. The energy change per unit time is the power dissipated at the junction. On the other hand, this power is the product of current and voltage. We conclude that the current in the junction is given by

$$I(\varphi) = -\frac{2e}{\hbar}\sum_p \frac{\partial E_p}{\partial \varphi} = \frac{e\Delta}{2\hbar}\sum_p \frac{T_p \sin\varphi}{\sqrt{1 - T_p \sin^2(\varphi/2)}}. \tag{1.172}$$

The supercurrent – or *Josephson* current – is an odd periodic function of the phase difference, and vanishes at $\varphi = 0$. In particular, for a tunnel junction $T_p \ll 1$, the supercurrent reads $I(\varphi) = I_c \sin\varphi$, where the amplitude $I_c = (e\Delta/2\hbar)\sum_p T_p = (\pi\Delta/2e)G_N$, where G_N is the conductance of the junction in the normal state. Here, I_c is the maximum possible supercurrent achieved at $\varphi = \pi/2$. Historically, the first superconducting junctions were tunnel ones. Usually, the term *Josephson junction* implies the above relation, between the current and phase, that corresponds to the Josephson energy $E_J(\varphi) = -E_J \cos\varphi$, $E_J = \hbar I_c/2e$. In principle, any nanostructure can serve as a Josephson junction; the current–phase characteristics essentially depends on the transmission eigenvalues. For example, a quantum point contact ($T_p = 1$) gives $I(\varphi) = I_c \sin(\varphi/2)$, $I_c = (\pi\Delta/e)G_N$ and maximum current is achieved at $\varphi = \pi$ (Fig. 1.53).

[7] Intuitively, one would include the spin degeneracy in the state count. This would be wrong: the sum is over orbital states. The reason is that the BdG equations provide a double set of solutions, as mentioned in Section 1.8.1.

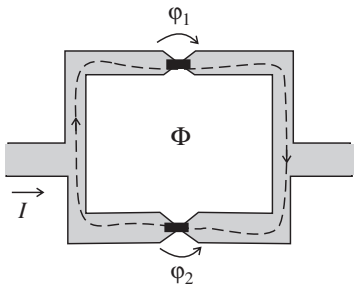

Fig. 1.54. The dc SQUID layout: two Josephson junctions with phase differences $\varphi_{1,2}$. The difference, $\varphi_1 - \varphi_2$, is determined by the flux Φ through the SQUID loop.

Exercise 1.20. Find the maximum supercurrent for a one-channel Josephson junction with transmission coefficient T. At which value of the phase is this current achieved?

The Josephson effect is essentially quantum-mechanical. We have already seen some examples of phenomena in which quantum mechanics plays an important role, such as the transmission through a double junction or the Andreev reflection from a single interface; in those cases, we were always able to present a classical analog of the effect to give them some meaning. In contrast, the Josephson effect is formulated in a way that cannot be interpreted classically: in classical physics, the phase of the wave function does not exist, and therefore a supercurrent cannot occur. The Josephson effect is one of the best illustrations of the concepts of quantum mechanics.

Josephson junctions are applied in many areas where a sensitive measurement of magnetic fields is an issue. Such a measurement is performed with a superconducting quantum interference device (SQUID). In the conceptually simplest version (dc SQUID), the device is a large superconducting loop with two arms intercepted by Josephson junctions (Fig. 1.54). The current through the device is the sum of the currents through both junctions, $I = I_1(\varphi_1) + I_2(\varphi_2)$, where we denote the phase drops at the junctions by φ_1 and φ_2, respectively.

Let us consider a magnetic field B applied perpendicular to the plane of the SQUID. The magnetic field modifies the phase drops at the junctions making them unequal. Indeed, the global gauge invariance requires that the phase and the vector potential always come in the combination $\nabla\varphi - (2e/\hbar c)\boldsymbol{A}$. Let us integrate this combination over the SQUID loop (the integration contour is given by the dashed curve in Fig. 1.54). In doing so, we can neglect the phase gradients in the bulk superconductors, but we must keep the phase drops at the Josephson junctions. This yields

$$\oint \mathrm{d}\boldsymbol{r}\,(\nabla\varphi - (2e/\hbar c)\boldsymbol{A}(\boldsymbol{r})) = \varphi_1 - \varphi_2 + 2\pi\,\Phi/\Phi_0,$$

where we have used the Stokes theorem transforming the contour integral of the vector potential to the area integral of the field – the magnetic flux Φ through the SQUID loop, $\Phi_0 = \pi\hbar c/e$ being the flux quantum (see Section 1.6). The phase shift along the closed contour is zero: $\varphi_1 - \varphi_2 = -2\pi\,\Phi/\Phi_0$.

Now we calculate the Josephson current in the SQUID, assuming equal tunnel Josephson junctions, $I = I_c(\sin\varphi_1 + \sin\varphi_2)$. Given the relation between the phase drops, we obtain

$$I = 2I_c \cos\left(\frac{\pi\Phi}{\Phi_0}\right) \sin\left(\varphi_2 + \frac{\pi\Phi}{\Phi_0}\right). \tag{1.173}$$

If we fix the total current I, the only independent parameter that can adjust to the current is the phase drop φ_2. However, this is only possible if the current I does not exceed $I_{\max} = 2I_c|\cos(\pi\Phi/\Phi_0)|$. Otherwise, the current is not a supercurrent and a finite voltage is measured on the SQUID. The area of the loop can be quite large, even of meter scale. Since the SQUID measures Φ, the total flux through the whole area of the loop, it is sensitive to astonishingly small magnetic fields.

Control question 1.24. Which magnetic field significantly changes the critical current of a SQUID with dimensions 1 m × 1 m?

Exercise 1.21. Consider a SQUID in which one of the junctions is of tunnel origin, $I_b(\varphi) = I_b \sin\ \varphi$ and another is characterized by $I_s(\varphi)$ to be determined from the measurement of the SQUID critical current. Assume $I_b \gg I_s$. (i) Show that, in zeroth order in I_s/I_b, the critical current does not depend on the flux. At which value of φ_b is this critical current achieved? (ii) Compute the critical current in the next order and explain how to recover $I_s(\varphi)$ from the measurement.

1.8.5 Superconducting junction at constant voltage bias

If a constant voltage V is applied across a superconducting junction, the phase difference increases linearly with time, $\varphi = (2eV/\hbar)t$. The junction between the two superconductors reacts to the constant voltage in a manner very different from junctions in the normal state: it produces an ac current (*ac Josephson effect*) that oscillates at the Josephson frequency $2eV/\hbar$.

If the voltage is low, $eV \ll \Delta$, the origin of the ac current is easy to comprehend. The linear sweep of the phase gives rise to the oscillating motion of the energies of the Andreev bound states. The ac current is given by Eq. (1.172), with $\varphi = (2eV/\hbar)t$. There is no dc current. The latter would imply the energy dissipation. However, the energies of all bound states return to the same position over a time period $\pi\hbar/eV$.

If the voltage eV is comparable with the value of the superconducting gap Δ, the situation is more complicated. Since the Josephson frequency is comparable with the energies of the states, we cannot expect that the energies adiabatically follow the time-dependent phase. Besides, there is a dissipation: the junction creates quasiparticles above the gap that leave the junction region carrying the energy away. Thus, we expect to observe a dc current.

To see how this works, let us first consider an open channel between two superconducting electrodes biased at finite constant voltage V. As already noted, the current does not actually depend on the spatial distribution of the voltage. We can assume that the voltage

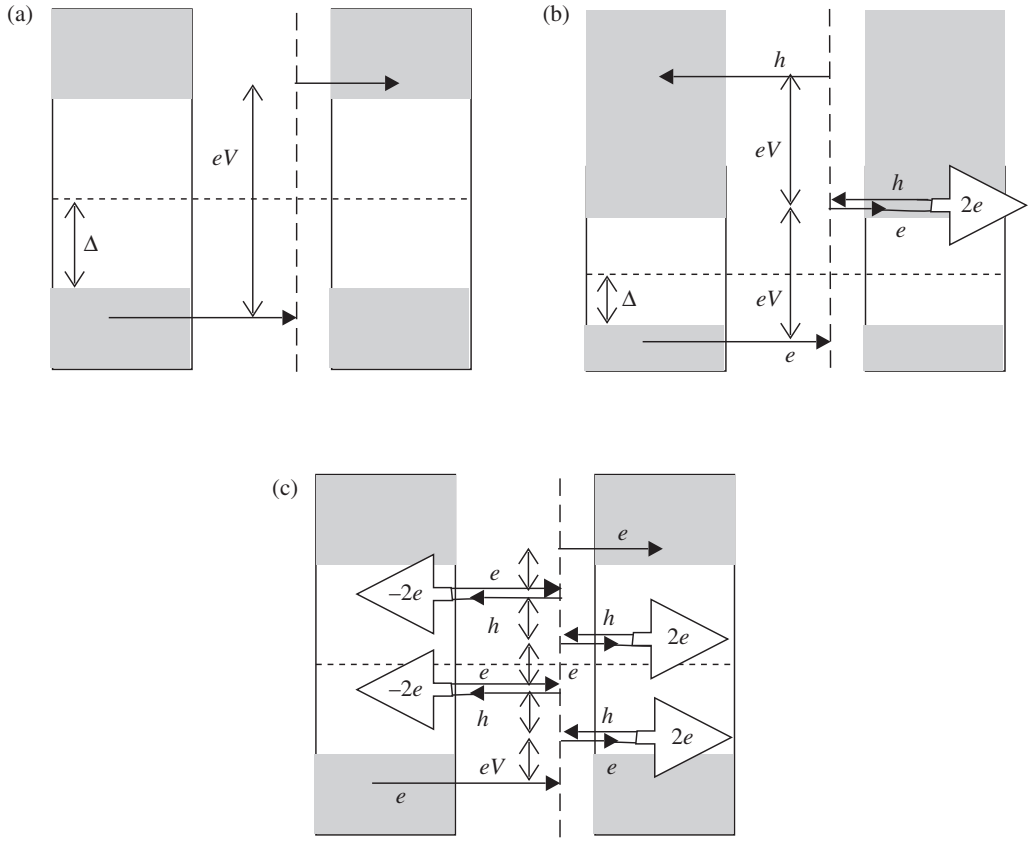

Fig. 1.55. **Elementary scattering processes in a voltage-biased open channel between two superconductors. Electrons (holes) acquire energy eV when crossing the dashed line from the left (right). Quasiparticle states are available in the shaded regions. (a) If $eV > 2\Delta$, a quasiparticle can be transferred from the left to the right in one shot. (b) Alternatively, it may be Andreev-reflected and get to the left at a higher energy. (c) Multiple Andreev reflections are required for such processes at $eV \ll \Delta$. The process shown transfers five elementary charges and is enabled at $5eV > 2\Delta$.**

drops over an arbitrary point of the channel (given by the dashed line in Fig. 1.55). When an electron (hole) crosses the point from the left to the right it increases (decreases) its energy by eV. It decreases (increases) the energy by the same amount while crossing from the right to the left. Since the energies are changing in the process of transmission, we cannot separate positive and negative energies in BdG equations as we did before and we consider quasiparticle energies of both signs. Then, in both left and right electrodes only quasiparticle states with $|E| > \Delta$ are available (Fig. 1.55). Let us consider an electron coming from the left superconducting electrode with an energy E slightly below $-\Delta$. It crosses the point where the voltage drops so it arrives at the right electrode with energy $E + eV$. If $E + eV > \Delta$, it may leave the junction, reaching the quasiparticle states available at this energy. This requires $eV > 2\Delta$. Thereby, the electron from negative energies has been transformed into a quasiparticle at positive energies. This can be seen as the generation of two quasiparticles of two *positive* energies: one with energy $-E > \Delta$ and another with $E + eV > \Delta$ (Fig. 1.55 (a)).

Control question 1.25. Compare the energies of the initial and final states. What charge is transferred through the junction in the course of the process?

Alternatively, the electron does not leave the junction but instead is converted into a hole at the superconducting electrode. The hole crosses the voltage drop from the right to the left, increasing its energy and arriving at the left electrode with energy $E + 2eV$. If it escapes to the left electrode, we have quasiparticles with energies $-E$ and $E + 2eV$, and the charge transferred through the junction equals $2e$. Otherwise, it is converted into an electron of the same energy. This brings us back to the beginning of the process: an electron incoming from the left. We conclude that Andreev reflections can help a process to result in any number of charges transferred, although only two quasiparticles are created. Since the probabilities of Andreev reflections (Eq. (1.162)) quickly decrease with increasing energy, the probabilities of the processes transferred with multiple charge are small.

This is quite different if the voltage is small, $eV \ll \Delta$. Let us again consider an incoming electron with energy E slightly below $-\Delta$. If $E + eV > -\Delta$, there are no available quasiparticle states in the right lead, and the electron has to turn into a hole by Andreev reflection. The hole arrives at the left lead with the slightly larger energy $E + 2eV < \Delta$, so Andreev reflection is the only option. The process of subsequent Andreev reflections continues until the energy of an electron or a hole exceeds Δ. We conclude that each such process transfers at least $2\Delta/eV$ elementary charges. Generally, at $eV \simeq \Delta$ we find the processes that differ in the charge transferred, en. The n-process involves $n-1$ Andreev reflections and starts at threshold voltage $eV_n > 2\Delta/n$. The onset of each process produces a singularity in I–V curves at the corresponding voltage. These singularities – subgap structure at I–V curves – form an experimental signature of these *multiple Andreev reflections*.

The quantitative theory should include the scattering between the superconducting electrodes. We sketch the general approach below [33, 34].

The setup is the same as the one used to calculate Andreev bound states. The important difference is that the amplitudes of the electrons and holes are not at the same energy: instead, the time-dependent amplitude is a superposition of all energies separated by eV, i.e.

$$\psi(t) = \sum_n \psi_n \mathrm{e}^{-\mathrm{i}(E+neV)t/\hbar}.$$

Each of the amplitudes ψ_n can describe incoming or outgoing electrons or holes. These amplitudes are related by the scattering matrix of the nanostructure,

$$\begin{pmatrix} \boldsymbol{b}_\mathrm{e} \\ \boldsymbol{b}_\mathrm{h} \end{pmatrix} = \begin{pmatrix} \hat{s} & 0 \\ 0 & \hat{s}^* \end{pmatrix} \begin{pmatrix} \boldsymbol{a}_\mathrm{e} \\ \boldsymbol{a}_\mathrm{h} \end{pmatrix}, \tag{1.174}$$

where, in distinction from Eq. (1.167), the amplitudes are shifted in energy by eV to incorporate the voltage drop,

$$\boldsymbol{b}_\mathrm{e} = \begin{pmatrix} b_{\mathrm{Le},n} \\ b_{\mathrm{Re},n+1} \end{pmatrix}; \quad \boldsymbol{b}_\mathrm{h} = \begin{pmatrix} b_{\mathrm{Lh},n} \\ b_{\mathrm{Rh},n-1} \end{pmatrix},$$

and similarly for $\boldsymbol{a}$.

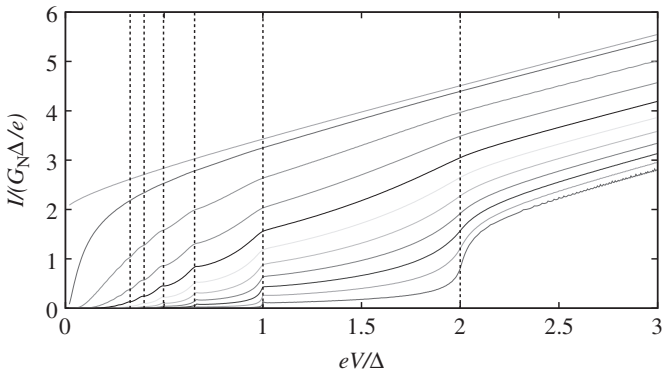

Fig. 1.56. ***I–V*** **curves of a single-channel superconducting junction. The transmission eigenvalue T_p increases from 0.1 (lowest curve) to 1 (upper curve) with step 0.1 except for the curve below the upper curve, for which $T_p = 0.98$. Vertical dotted lines indicate threshold voltages V_1–V_6.**

Let us consider a scattering state for the case when a quasiparticle with energy $E < -\Delta$ comes from the left superconducting electrode. At the left superconductor, the energy of electrons and holes stays the same. The corresponding complementary relation for $\boldsymbol{a}$, $\boldsymbol{b}$ does not mix the amplitudes of different energies (different n),

$$\begin{pmatrix} a_{\mathrm{Le},n} \\ a_{\mathrm{Lh},n} \end{pmatrix} = \begin{pmatrix} 0 & r_{\mathrm{A}}^{(n)} \\ r_{\mathrm{A}}^{(n)} & 0 \end{pmatrix} \begin{pmatrix} b_{\mathrm{Le},n} \\ b_{\mathrm{Lh},n} \end{pmatrix} + \begin{pmatrix} u(E) \\ v(E) \end{pmatrix} \delta_{n0}, \tag{1.175}$$

where the Andreev reflection amplitudes $r_{\mathrm{A}}^{(n)}$ are taken at corresponding energies $E_n = E + eVn$ and are given by Eqs. (1.161) and (1.162). We disregard the dependence of the amplitudes on the superconducting phase since the superconducting phase difference is already taken into account by the voltage drop between the electrodes. We can thus conveniently set both $\varphi_{\mathrm{R,L}}$ to 0. The second term in Eq. (1.175) accounts for the incoming quasiparticle at energy E (hence $n = 0$). We learn from Appendix B that a quasiparticle excitation is a superposition of an electron and a hole, with $u, v = ((1 \pm \sqrt{1 - (\Delta/E)^2})/2)^{1/2}$ being the superposition coefficients. The amplitude of the incoming quasiparticle enters the equations for a_n and b_n as a free term. Similar relations hold at the right superconductor. Since no quasiparticle comes from the right, one has simply

$$\begin{pmatrix} a_{\mathrm{Re},n} \\ a_{\mathrm{Rh},n} \end{pmatrix} = \begin{pmatrix} 0 & r_{\mathrm{A}}^{(n)} \\ r_{\mathrm{A}}^{(n)} & 0 \end{pmatrix} \begin{pmatrix} b_{\mathrm{Re},n} \\ b_{\mathrm{Rh},n} \end{pmatrix}. \tag{1.176}$$

The scattering state is found by solving the resulting (in principle, infinite) system of equations for a_n, b_n. The solution is cumbersome and has to be analyzed numerically. Each scattering state, with quasiparticles coming either from the left or from the right at all negative energies, provides a contribution to the current that is obtained by integration over all energies. The result is a function of the ratio eV/Δ and of the transmission coefficient T_p in the channel, $I_p = (G_{\mathrm{Q}}\Delta/e)\mathcal{I}(eV/\Delta, T_p)$ (Fig. 1.56). The total current is the sum over all transmission channels.

We note that $\mathcal{I}$ is strongly suppressed below the voltage $2\Delta/e$ if $T_p \ll 1$. Indeed, the charge transfer below this threshold requires at least one Andreev reflection. To perform this, the electron or hole should traverse the scattering region one more time. The probability of this is suppressed by a factor T_p. Similarly, the charge transfer below V_n requires n Andreev reflections and is suppressed by a factor T_p^n. At large voltages $eV \gg \Delta$, the superconductivity is not important for charge transfer, and current approaches its value in normal metal, $\mathcal{I} \simeq T_p(eV/\Delta)$. In principle, there are singularities in I–V curves at each threshold voltage V_n corresponding to the onset of a process with charge en transferred. The singularities are clearly visible up to $T_p \simeq 0.7$. In the tunneling regime, the singularities are steps (see Section 3.7.2, Eq. (3.102)) that are increasingly rounded upon increasing T_p. The actual singularities that survive the rounding, even at $T_p \to 1$, are jumps of the second derivative of the current and are not visible with the naked eye.

Beside the dc current, the scattering approach allows us to find the harmonics I_m of the ac current at multiples of the Josephson frequency, $I(t) = \sum_m I_m \exp(2eVtm/\hbar)$ [34]. Indeed, each scattering state contributes to the time-dependent current, given by

$$I(t) \propto \left(|\psi_{\mathrm{e}}(\boldsymbol{r},t)|^2 - |\psi_{\mathrm{h}}(\boldsymbol{r},t)|^2\right),$$

where $\psi_{\mathrm{e,h}}$ are electron and hole components of the amplitude. Substituting the time-dependent amplitudes, we see that

$$I_m \propto \sum_n \left(b^*_{\mathrm{Le},n} b_{\mathrm{Le},n+m} - b^*_{\mathrm{Lh},n} b_{\mathrm{Lh},n+m} - a^*_{\mathrm{Le},n} a_{\mathrm{Le},n+m} + a^*_{\mathrm{Lh},n} a_{\mathrm{Lh},n+m}\right).$$

The harmonics also exhibit subgap singularities at $V = V_n$.

It is clear that the processes involving a transfer of multiple charges should lead to interesting and non-trivial full counting statistics; this has been analyzed in Ref. [35] in detail. As we have seen, at low voltages and transmissions, an elementary process of charge transfer involves the transfer of many ($\simeq 2\Delta/eV$) elementary charges. To make an analogy, the electrons do not traverse the nanostructure as separate independent vehicles; rather, they are organized in long trains of $\simeq 2\Delta/eV$ coaches. This enhances the Fano factor, and accounts for its large values. This enhancement has been confirmed experimentally [36] for nanostructures with a well controlled set of the transmissions T_p.

1.8.6 Nanostructure pin-code: experimental

We have already mentioned many times that the scattering and transport properties of a nanostructure are completely determined by the full set of transmission eigenvalues, known as the "pin-code." It is very difficult to crack the pin-code in the course of measurement in the normal state since the Landauer conductance gives only the sum of all T_p. On the contrary, the I–V curves of a superconducting junction are reasonably sensitive to individual eigenvalues T_p. The brilliant experiment described in Ref. [37] demonstrates how one can extract all the relevant transmission eigenvalues just by measuring the I–V curves.

The experiments were performed with superconducting break junctions. In the break junction technique [38], a long and narrow wire is deposited on an elastic substrate. In the

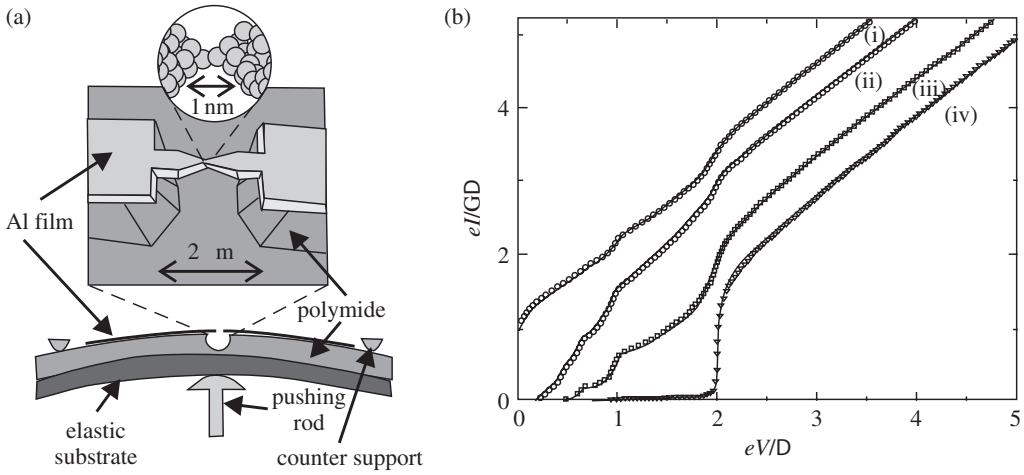

Fig. 1.57. **Experimental determination of nanostructure pin-code [37] (a) Break junction: experimental layout. (b) A fit of I–V curves in the superconducting state reveals the individual transmission eigenvalues. (i) $T_1 = 0.997, T_2 = 0.46, T_3 = 0.29$; (ii) $T_1 = 0.74, T_2 = 0.11$; (iii) $T_1 = 0.46, T_2 = 0.35, T_3 = 0.007$; (iv) T_1 = 0.0025.**

course of the experiment, the substrate is bent so that the wire stretches and eventually breaks; hence the name "break junctions." The substrate bending can be controlled with high precision, so that it is possible to stabilize the system immediately before the wire breaks. At this moment, the narrowest place of the wire is only several atoms wide, and the voltage drops at narrowest place. Thereby one creates an atomic-size nanostructure with a few open transport channels. One monitors the conductance during the experiment and tunes the nanostructure to any desired value of G.

The samples used in Ref. [37] were suspended aluminum microbridges (Fig. 1.57), 2 μm long and 100 nm thick, constricted in the middle to approximately 100 nm. This is still too wide for a few-channel junction, and further narrowing of the constriction has been achieved with the break junction technique. From both sides, the bridge opens to large (dozens of microns long) pads glued to an elastic organic (polyamide) substrate. The substrate was mounted on a bending mechanism, which was adjusted in such a way that a micron-long displacement of the mechanism resulted in a well controlled change in the distance between the clamping points of the bridge of only 0.2 nm. The samples were first broken and then brought back into contact to form a nanostructure with a few open transport channels. The experiment was performed at ultra-low temperature ($\sim$ 1 mK, well below the temperature of the superconducting transition). In the course of the experiment, the clamping points were slowly pushed apart. This diminishes, and effectively reduces the number of, transmission eigenvalues: the conductance goes down. The setup was stable enough that the deformation could be stopped at any point (corresponding to a particular set of transmission eigenvalues) and the dc current versus the applied voltage could be measured at this point.

Fitting the I–V curves using a sum of contributions of individual transport channels, one can very precisely determine all the relevant transmission eigenvalues. The number of transmissions T_p taken into consideration is determined by the accuracy of the fit, and

the authors were able to resolve up to the five biggest transmission eigenvalues. Examples of similar fits are presented in Fig. 1.57, where we see the precision of the fits and of the transmission eigenvalues extracted.

The importance of these experiments on superconducting break junctions goes far beyond an experimental check of validity of the theory of non-equilibrium transport in Josephson junctions. The experiments provide an experimental justification of the basics of scattering theory of quantum transport.

1.9 Spin-dependent scattering

Electrons have spin 1/2. This implies that the electron wave function is a two-component quantity – a *spinor*, given by

$$\psi(\boldsymbol{r}) = \begin{pmatrix} \psi_\uparrow(\boldsymbol{r}) \\ \psi_\downarrow(\boldsymbol{r}) \end{pmatrix},$$

where $\psi_{\uparrow(\downarrow)}$ correspond to the states with spin "up" ("down") with respect to a given axis. Spin is a physical quantity, very much like electric charge or momentum. It has three components x, y, and z, making a pseudovector. The corresponding operator is expressed in terms of the pseudovector of 2×2 *Pauli matrices* $\hat{\boldsymbol{\sigma}}$, $\hat{\boldsymbol{S}} = \hbar\hat{\boldsymbol{\sigma}}/2$ that act on spinors. Frequently, electron spin can be disregarded, as we have been doing so far. In the absence of interactions that explicitly depend on spin, the wave functions $\psi_\uparrow$ and $\psi_\downarrow$ are identical. The only fact to take into account is that the number of electron states is twice that without spin. In quantum transport, this only leads to the factor 2_s in the conductance quantum. In this section, we consider circumstances in which the spin-dependent interactions cannot be disregarded. This may happen due to three factors: spin-splitting in a magnetic field, interaction with an exchange field in ferromagnets, and spin-orbit interaction. All these factors can be incorporated into the scattering matrix, making it spin-dependent.

Zeeman splitting

A magnetic field $\boldsymbol{B}$ does many things to electrons: it produces phase shifts (described in Section 1.6), and it also tries to bend electron trajectories into Larmor circles. These *orbital* effects will be disregarded in this section. The magnetic field also interacts with electron spin, so that the spin-dependent Hamiltonian reads $\hat{H} = g\mu_\mathrm{B}\boldsymbol{B}\cdot\hat{\boldsymbol{\sigma}}/2$. Here the combination of fundamental constants $\mu_\mathrm{B} = e\hbar/2mc$ is the Bohr magneton, and $g = 2$ for electrons in a vacuum. In semiconductor heterostructures, the value of this g-factor may be significantly modified and even change sign; for example, $g = -0.44$ for electrons in bulk GaAs. Thus, the energy of the state with the spin projection parallel (antiparallel) to the magnetic field is shifted up (down) by $g\mu_\mathrm{B}B/2$. This is known as *Zeeman splitting*. To understand the effect of this splitting on quantum transport, let us recall the model of an adiabatic wave guide (Section 1.2) that describes a quantum point contact. Within each transport channel n, the electrons with the spin projection $\pm\hbar/2$ (spin up and spin down) feel different effective potential energies, given by